*Journal of Sound and Vibration* (1998) **211**(4), 716–727

# IMPEDANCE CHARACTERISTICS OF ACTIVE INTERIOR NOISE CONTROL SYSTEMS

V. Jayachandran and J. Q. Sun

*Department of Mechanical Engineering, University of Delaware, Newark, DE* 19716, *U.S.A.*

(*Received* 26 *March* 1997, *and in final form* 27 *October* 1997)

## 1. INTRODUCTION

Over the past two decades, significant progress has been made in quieting aircraft and automobile interiors by using advanced control theory, and modern sensor and actuator technologies. In this context, the active control of harmonic low frequency noise has received considerable attention. Active noise cancellation (ANC) is a popular method for such control applications [1–5]. This method relies on injecting into the domain to optimally minimize a global performance measure, e.g., the acoustical potential energy of the system. The sound field is monitored through microphones and this information is fed back to drive the secondary acoustic sources such as loudspeakers in an attempt to reduce the mean pressure in the three-dimensional domain. ANC does not attempt to change the vibration characteristics of the primary structural sources. The pressure field introduced by the control modifies the structural–acoustic interaction of the vibrating boundaries with the acoustic domain. This method is usually applied at low frequencies where the model density is low and passive methods do not work well due to long acoustic wavelength.

Another technique for noise control is absorption. Sound absorption occurs when the impedance of an absorbing medium such as an active foam or trim panel matches the impedance of the acoustic medium. Passive sound absorption technologies have been extensively used in a broad range of applications including automobiles and aircraft cabins. Although this technique is generally passive and is typically used for suppressing high frequency noise, one can envisage a system for controlling middle range frequency sound where the mechanical impedance of the acoustic actuators is actively adjusted to match that of the acoustic medium in order to maximize absorption. Indeed, active sound absorption has been studied by many researchers. Extensive studies of active sound absorption are reported in references [6–9]. A one dimensional active acoustic sink has been developed for wide band noise control in reference [10]. Darlington and Avis have studied this subject [11] and Darlington has formulated some interior noise control algorithms in terms of acoustic impedance [12]. The principle of motional feedback has been applied to active acoustic materials to achieve an adjustable reflection coefficient for controlling reverberation in a room [13]. Guicking and Karcher have developed an active impedance control system for one-dimensional plane waves at normal incidence in which they control the reflection coefficient of a loudspeaker [14]. Active sound absorption of the open field has been studied based on the "$\lambda/4$ resonance absorber" principle in reference [15].

Even though there has been much work on sound absorption, studies on impedance conditions of active noise control systems in three-dimensional enclosures are rare. Theoretical expressions have been analytically derived for the "optimal" secondary source impedance only in the case of the control of one-dimensional sound in a duct. One of the latest studies is that by Lacour *et al*. [16] in which they obtain an analytical expression

0022–460X/98/140716 + 12 $25.00/0/sv971381 

for the optimal secondary source impedance in a one-dimensional situation and then try to extend the results to a three-dimensional problem by enforcing similar impedance values at the control source. The unpredictability of the results indicates that the multi-dimensional problem is clearly more complex and requires a full fledge three-dimensional study to understand the impedance conditions at the secondary sources in order to apply active impedance control techniques. Unlike the simple one-dimensional case where analytical expressions for the field variables are easily derived, the three-dimensional study must be performed numerically.

In order to study the feasibility of using such active impedance control schemes, a numerical study of impedance conditions at the primary and control sources of an active noise control system in a three-dimensional enclosure has been performed. The optimal control solution is determined using the acoustic boundary control concept [17–19]. A qualitative and quantitative analysis of the acoustic medium's impedance before and after active control is presented in this paper. The effect of primary source strengths and locations on the control solution has been studied in detail. A modal model is used in the simulations. The study in this paper provides a better understanding of the physics of the problem and suggests performance upper bounds for semi-active or active sound absorption in three-dimensional enclosures.

The remainder of this paper is organized as follows. In section 2 the mathematical model for the numerical simulation is discussed. In section 3 an analysis of the impedance field in the enclosure along with numerical simulation results is presented. The paper is concluded in section 4.

## 2. ANALYTICAL MODELLING

Consider a three-dimensional cuboidal enclosure with dimensions $a$, $b$ and $c$ along the $x$, $y$ and $z$ axes. Figure 1 shows a schematic of the physical system being modelled. The wall at $x = a$ is modelled as a simply supported plate vibrating harmonically. There are also interior noise sources present in the enclosure. The vibrating wall and the interior sources act as primary sources of acoustic disturbances. Consider a harmonic sound field where all sources are assumed to be operating at the same frequency. Hence, the pressure field is governed by the inhomogeneous Helmholtz equation,

$$(\nabla^2 + \kappa^2)p(\mathbf{r}) = -\mathrm{j}\rho\omega q_{vol}(\mathbf{r}), \tag{1}$$

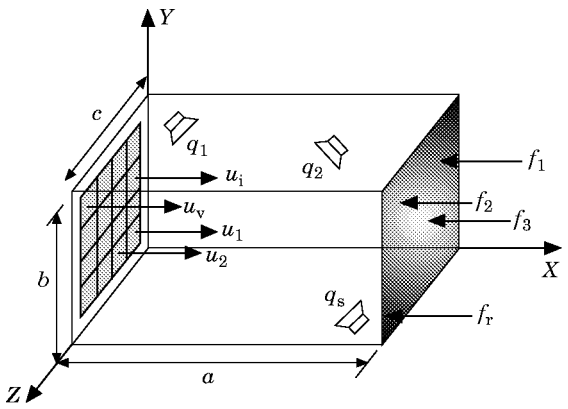


Figure 1. The three dimensional rectangular enclosure.

where $p(\mathbf{r}, t) = p(\mathbf{r})\, e^{j\omega t}$ is the acoustic pressure, $\mathbf{r} = \{x, y, z\}$ is the position vector, $\kappa = \omega/c_0$ is the acoustic wavenumber, $c_0$ is the speed of sound and $\rho$ is the density of the air. The interior acoustic source distribution is given by $q_{vol}(\mathbf{r}, t) = q_{vol}(\mathbf{r})\, e^{j\omega t}$. When all the enclosure walls are rigid, the boundary conditions at $x = 0$, $a$, $y = 0$, $b$ and $z = 0$, $c$ are homogeneous and of the Neumann type. These boundary conditions can be modified, depending on the location of the primary structural source and the boundary control sources. In case of the system under study, the primary structural source is located at $x = a$. Also, a grid of control sources consisting of vibrating rigid rectangular pistons is located at $x = 0$. The boundary conditions in the $x$ direction are hence inhomogeneous and given by

$$\partial p/\partial x(0) = -j\rho\omega u(y, z), \qquad (\partial p/\partial x)(a) = -j\rho\omega w(y, z), \tag{2}$$

where $u(y, z)$ is the velocity distribution on the control surface, and $w(y, z)$ is the velocity distribution on the surface of the vibrating wall. Following the solution technique discussed in reference [20], the pressure field due to the wall vibration can be obtained as

$$p_w(\mathbf{r}) = \sum_{m=0}^{\infty}\sum_{n=0}^{\infty}\left[\frac{x^2}{2a} + \sum_{l=0}^{\infty}\gamma_{lmn}\cos\left(\frac{l\pi x}{a}\right)\right]W_{mn}\cos\left(\frac{m\pi y}{b}\right)\cos\left(\frac{n\pi z}{c}\right), \tag{3}$$

where

$$\gamma_{lmn} = \begin{cases} -a/6 - 1/a(\kappa^2 - \kappa_{lmn}^2), & l = 0, \\ -(2a(-1)^l/l^2\pi^2)\,([\kappa^2 - \kappa_{omn}^2]/[\kappa^2 - \kappa_{lmn}^2]), & l > 0, \end{cases} \tag{4}$$

and

$$\kappa_{lmn}^2 = \omega_{lmn}^2/c_0^2 = [l\pi/a]^2 + [m\pi/b]^2 + [n\pi/c]^2. \tag{5}$$

The pressure field due to interior sources is given by

$$p_q(\mathbf{r}) = \sum_{l=0}^{\infty}\sum_{m=0}^{\infty}\sum_{n=0}^{\infty}\frac{Q_{lmn}}{\kappa^2 - \kappa_{lmn}^2}\cos\left(\frac{l\pi x}{a}\right)\cos\left(\frac{m\pi y}{b}\right)\cos\left(\frac{n\pi z}{c}\right), \tag{6}$$

where

$$Q_{lmn} = \varepsilon_{lmn}^2\sum_{i=1}^{s} q_i\cos\left(\frac{l\pi x_i}{a}\right)\cos\left(\frac{m\pi y_i}{b}\right)\cos\left(\frac{n\pi z_i}{c}\right). \tag{7}$$

Here $\varepsilon_{lmn}$ are normalization constants for the mode functions and $q_i$ represents the strength of the $i$th source. Finally, the pressure field due to the controlled sources is given by

$$p_u(\mathbf{r}) = \sum_{m=0}^{\infty}\sum_{n=0}^{\infty}\left[-\frac{(a-x)^2}{2a} + \sum_{l=0}^{\infty}\beta_{lmn}\cos\left(\frac{l\pi x}{a}\right)\right]U_{mn}\cos\left(\frac{m\pi y}{b}\right)\cos\left(\frac{n\pi z}{c}\right), \tag{8}$$

where

$$\beta_{lmn} = \begin{cases} a/6 + 1/a(\kappa^2 - \kappa_{lmn}^2), & l = 0, \\ (2a/l^2\pi^2)\,([\kappa^2 - \kappa_{omn}^2]/[\kappa^2 - \kappa_{lmn}^2]), & l > 0, \end{cases} \tag{9}$$

and

$$-j\rho\omega u(y, z) = \sum_{m=0}^{\infty} \sum_{n=0}^{\infty} U_{mn} \cos\left(\frac{m\pi y}{b}\right) \cos\left(\frac{n\pi z}{c}\right). \tag{10}$$

The coefficient $U_{mn}$ is obtained as

$$U_{mn} = \sum_{i=1}^{v} U_{mn}^{i} u_i,$$

where $u_i$ is the velocity of the $i$th piston and $U_{mn}^{i}$ is a coefficient depending on the geometry and location of the piston. The total pressure in the enclosure is given by a superposition of the individual contribution as

$$p(\mathbf{r}) = p_w(\mathbf{r}) + p_q(\mathbf{r}) + p_u(\mathbf{r}). \tag{11}$$

The velocity at any point in the acoustic medium may be directly determined from the pressure as

$$\mathbf{u}(\mathbf{r}) = -(1/\mathrm{j}\omega\rho)\nabla p(\mathbf{r}) \equiv \{u_x, u_y, u_z\}^{\mathrm{T}}. \tag{12}$$

The expressions for pressure and velocity can be used for determining the specific acoustic impedance at any point in the medium as [21, 22]

$$z(\mathbf{r}) = p(\mathbf{r})/|\mathbf{u}(\mathbf{r})|. \tag{13}$$

The acoustic impedance at any section $x = x_0$ is determined as a slightly modified version of that defined in reference [21]. The authors define it as

$$\bar{z}(x_0) = \sqrt{\int_0^b \int_0^c |p(x_0, y, z)|^2 \, \mathrm{d}y \, \mathrm{d}z \Big/ \int_0^b \int_0^c |u_x(x_0, y, z)|^2 \, \mathrm{d}y \, \mathrm{d}z}. \tag{14}$$

This expression is just a scaled version of the acoustic impedance and is used because it also gives a mean measure of the specific impedance over the surface. This may be compared with the pointwise specific acoustic impedance at the section.

The vibrating wall is modeled as a plate with simply supported edges under the excitation of harmonic point forces. Hence, for $r$ point forces, $f_i$ acting on the plate, one can write

$$p_w(\mathbf{r}) = \sum_{i=1}^{r} x_{f_i}(\mathbf{r}, \mathbf{r}_i, \omega) f_i \equiv x_f^{\mathrm{T}} \mathbf{f}, \tag{15}$$

where $x_{f_i}$ is the coupling coefficient between the pressure field and the $i$th point force located at $\mathbf{r}_i$, and $\mathbf{x}_f = \{x_{f_1}, x_{f_2}, \ldots, x_{f_r}\}^{\mathrm{T}}$, $f = \{f_1, f_2, \ldots, f_r\}^{\mathrm{T}}$. Similarly, the pressure field due to the $s$ internal sources in the enclosure may be written as

$$p_q(\mathbf{r}) = \sum_{j=1}^{s} z_{q_j}(\mathbf{r}, \mathbf{r}_j, \omega) q_j = \mathbf{z}_q^{\mathrm{T}} \mathbf{q}, \tag{16}$$

and the pressure field due to the control sources may be written as

$$p_u(\mathbf{r}) = \sum_{k=1}^{v} z_{u_k}(\mathbf{r}, \mathbf{r}_k, \omega) u_k = \mathbf{z}_u^{\mathrm{T}} \mathbf{u}. \tag{17}$$

The total pressure in matrix form is now given by

$$p(\mathbf{r}) = \mathbf{x}_f^{\mathrm{T}}\,\mathbf{f} + \mathbf{z}_q^{\mathrm{T}}\,\mathbf{q} + \mathbf{z}_u^{\mathrm{T}}\,\mathbf{u}. \tag{18}$$

The optimal control vector is obtained from the necessary condition for minimization of the enclosure time averaged acoustical potential energy:

$$J[u(y, z), w(y, z)] = \int_V p(\mathbf{r})p^*(\mathbf{r})\,\mathrm{d}V, \tag{19}$$

where $V$ denotes the volume of the enclosure and $p^*(\mathbf{r})$ is the complex conjugate of $p(\mathbf{r})$. One chooses to minimize the acoustical potential energy because it leads to a reduction of the mean pressure level, and also often leads to a reduction of the primary source power output. On the other hand, minimization of the source power output has been shown to not guarantee reducing the mean pressure [4]. The cost function may now be written in the following matrix form [4]:

$$J = \mathbf{u}^H\mathbf{A}\mathbf{u} + \mathbf{u}^H\mathbf{a} + \mathbf{a}^H\mathbf{u} + J_0, \tag{20}$$

where

$$\mathbf{A} = \int_V \mathbf{z}_u^*\,\mathbf{z}_u^{\mathrm{T}}\,\mathrm{d}V, \qquad \mathbf{a} = \int_V \mathbf{z}_u^*\,(\mathbf{z}_q^{\mathrm{T}}\,\mathbf{q} + \mathbf{z}_f^{\mathrm{T}}\,\mathbf{f})\,\mathrm{d}V,$$

$$J_0 = \int_V (\mathbf{q}^{\mathrm{T}}\mathbf{z}_q^* + \mathbf{f}^{\mathrm{T}}\mathbf{z}_f^*)\,(\mathbf{z}_q^{\mathrm{T}}\,\mathbf{q} + \mathbf{z}_f^{\mathrm{T}}\,\mathbf{f})\,\mathrm{d}V. \tag{21}$$

The optimal control vector is then determined from $\partial J/\partial\mathbf{u} = 0$ as

$$\mathbf{u}_{opt} = -\mathbf{A}^{-1}\mathbf{a}. \tag{22}$$

This expression may be used to find the optimal velocities for the actuators. Note that for a given number and arrangement of actuators, the matrix $\mathbf{A}$ is fixed. Hence, the optimal control velocities vary with the vector $\mathbf{a}$. Once the optimal control vector has been determined, the impedance field may be obtained using equations (13) or (14).

## 3. NUMERICAL SIMULATIONS

The simulations are carried out for a cuboidal enclosure of dimensions 1.1, 1.2 and 1.3 meters in the $x$, $y$ and $z$ directions, respectively. The vibrating wall is made of aluminum. The acoustic boundary control elements consist of a $2 \times 2$ grid of rectangular pistons [17–19]. The simulations are performed for the frequency range of 120 to 220 Hz which covers a region of low modal density.

### 3.1. *Optimal control solution*

One starts by looking at the enclosure mean pressure reduction due to control. The system is simulated in the presence of structural and interior sources separately. Figure 2 shows the mean interior pressure before and after control when only interior sources are present. The acoustic resonances can be easily spotted as the peaks in the mean pressure before control. The reduction in sound level after control is very good and the resulting profile is smooth and uniform. Figure 3 shows the same results for the case when only structural disturbances are present. The noise level reduction is again quite good at the

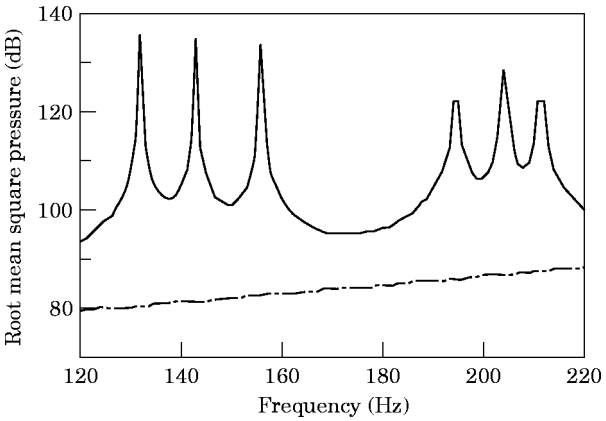


Figure 2. Enclosure mean pressure before and after control in the presence of interior acoustic source only: ——, before control; — - —, after control.

acoustic resonances, but the control is not as effective at the structural resonance frequencies.

3.2 *Impedance at the vibrating wall*

The impedance in the vicinity of the vibrating side wall before and after control is studied next. The acoustic impedance on the vibrating surface as defined in equation (14) is determined for a range of frequencies. Let us look at the case when only structural disturbances are present. Figure 4 shows a plot of the acoustic impedance at the wall as a function of frequency. The impedance drops to an almost flat profile after control, indicating a lower acoustic power output since the side wall velocity is assumed to be unchanged after control. This assumption is motivated by the practical situation on an aircraft where the fuselage is in a forced vibration condition that is not affected by acoustic controls in the cabin. Hence, the control action has achieved a noise reduction by unloading the side wall and effectively reducing its acoustic power output. An interesting quantitative observation that can be made in this case is that irrespective of the impedance conditions at the wall before control, the impedance profile after control is almost flat and is close to 200 $kg/m^2s$. Figure 5 shows a sample spatial profile for the pressure at the

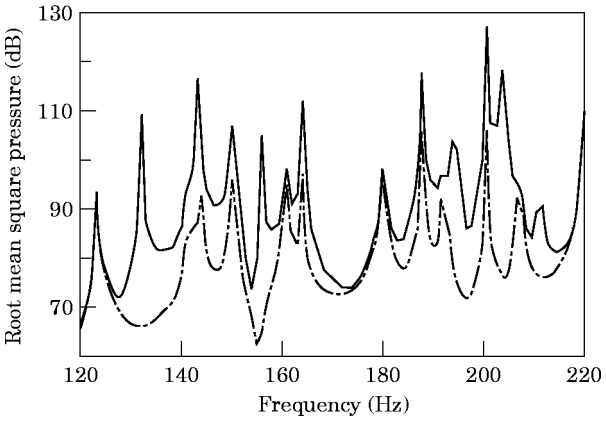


Figure 3. Enclosure mean pressure before and after control in the presence of structural disturbances only: ——, before control; — - —, after control.

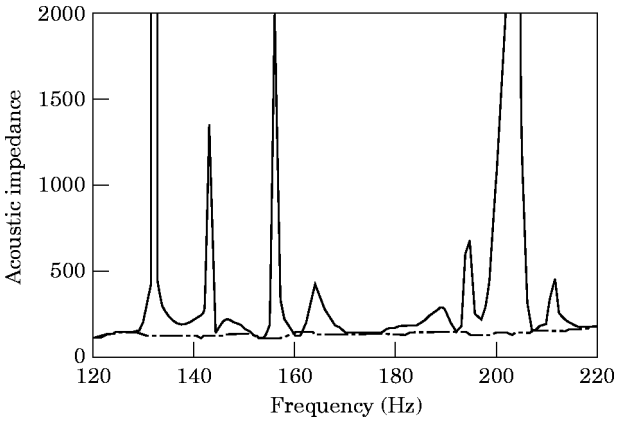


Figure 4. Acoustic impedance at the vibrating wall before and after control: ——, before control; — - —, after control.

vibrating wall before and after control at 200 Hz. One observes a large decrease in the sound pressure level after control. Since the velocity field at the wall remains the same, the pointwise specific acoustic impedance near the wall is also decreased by the same factor. This observation is in agreement with the discussion on cancellation of acoustic primary sources in reference [4].

### 3.3. *Impedance at the acoustic sources*

The impedance at the interior acoustic sources is studied next. Point sources are placed at different locations within the enclosure, and the pressure at these points before and after control is obtained for a range of frequenices. The volume velocity of these sources is assumed not to be affected by the control. This is a realistic assumption for the fuselage cabin where the interior acoustic source may be the air-conditioning system, for example. Its operation will not be changed by the action of acoustic controls. The cases for a single source and multiple sources are studied separately. In both cases, it has been observed that even though the mean pressure in the enclosure goes down due to the control action, this does not guarantee the same would happen for the local pressure at the primary point

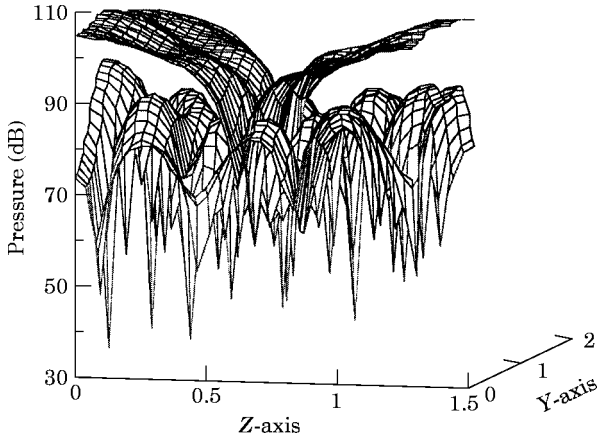


Figure 5. Pressure profile at the vibrating wall before (upper surface) and after (lower surface) control at 200 Hz.

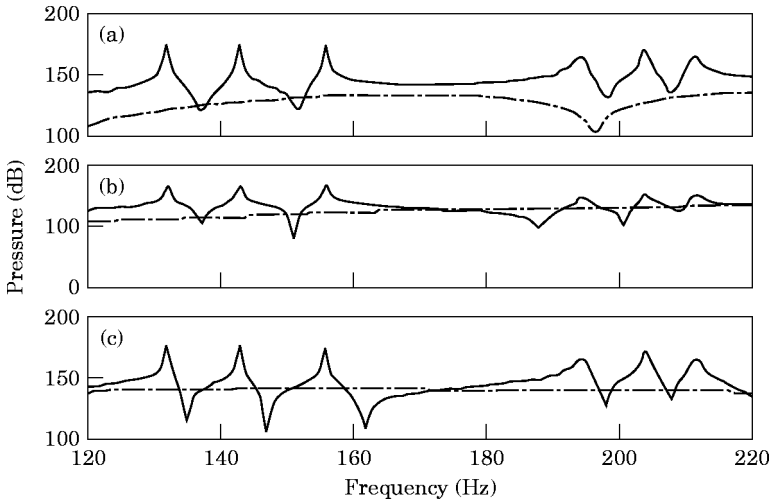


Figure 6. Pressure versus frequency at three point acoustic source locations. (a): $q = 0{\cdot}0008$ m$^3$/s, $r = (0{\cdot}11$ m, $0{\cdot}12$ m, $0{\cdot}13$ m); (b): $q = 0{\cdot}008$ m$^3$/s, $r = (0{\cdot}66$ m, $0{\cdot}72$ m, $0{\cdot}78$ m); (c): $q = 0{\cdot}08$ m$^3$/s, $r = (0{\cdot}99$ m, $1{\cdot}08$ m, $1{\cdot}17$ m). ——, Before control; — - —, after control.

source locations. Figure 6 shows the pressure before and after control at three point sources of strengths $0{\cdot}0008$ m$^3$/s and $0{\cdot}008$ m$^3$/s and $0{\cdot}08$ m$^3$/s, located at ($0{\cdot}11$ m, $0{\cdot}12$ m, $0{\cdot}13$ m), ($0{\cdot}66$ m, $0{\cdot}72$ m, $0{\cdot}78$ m) and ($0{\cdot}99$ m, $1{\cdot}08$ m, $1{\cdot}17$ m), respectively. One can see that the pressure, and hence impedance, does not necessarily drop at these locations for all the frequencies. Note that in this case, the mean enclosure pressure before and after control has a profile similar to that shown in Figure 2.

In general, the optimal control minimizes the total acoustic potential energy resulting in a more smooth pressure distribution in the enclosure. As a result, some points sitting at the pressure nodes or valleys before control may experience a sound level increase while the sound pressure is reduced at peak locations. If an interior point source is located near a pressure node, the impedance at that point may indeed be increased by the control. An increase in impedance at the constant volume velocity source implies larger acoustic power output from it. This phenomenon has not been discussed extensively before in the literature. Since the optimal control reduces the overall pressure, this phenomenon suggests that the increased power output of the primary source may be used to help reduce the pressure at some other locations where the control action may have inadvertently increased the pressure.

### 3.4. *Impedance at the control actuators*

One now considers the impedance on the surface of the control elements. This case is of special significance since it provides insight into the possibility of using active impedance control for noise suppression. First the case when the primary noise is purely structural is considered. One would like to examine the effect of the number and strength of the point forces driving the structure on the acoustic impedance at the control surface. Figure 7 shows the acoustic impedance versus frequency after control at the control surface when the side wall is driven by four different sets of forces. It was observed via numerous simulations that these profiles change only by small amounts as the amplitude and spatial distribution of the forces on the wall is varied. This implies that the overall control solution does not change much with the distribution as well as intensity of excitations on the side wall. This is an interesting result, and may be explained as follows. The forces acting on

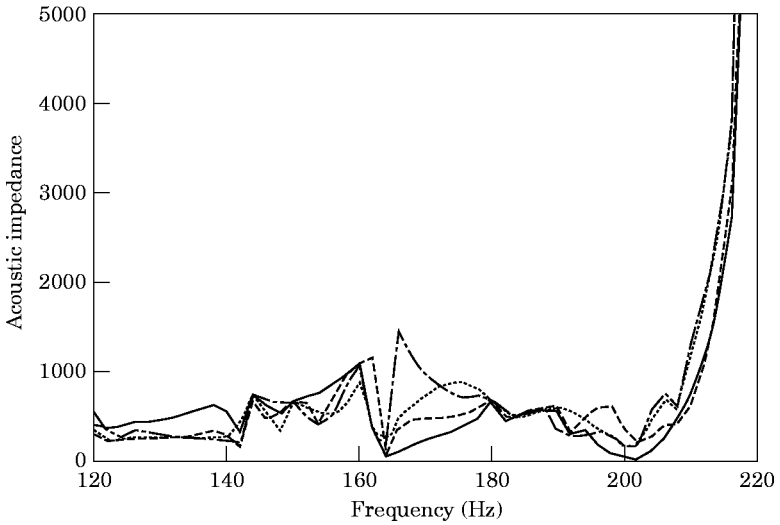


Figure 7. Acoustic impedance on the control surface after control in the presence of structural disturbances only. Different line types are for different force vectors.

the side wall pass through two modal filtering operations, i.e., the spatial information of the forces is filtered by two sets of dissimilar eigenfunctions when they contribute to the sound field. Therefore, the spatial information of the forces contained in the sound field is significantly attenuated and the optimal control as well as the resulting impedance in front of the control surface is quite insensitive to changes in the force amplitudes and distribution.

On the other hand, this is not true in case of interior sources. The profile of the acoustic impedance on the control surface versus frequency is observed to change significantly as the source strengths and locations are changed. This is to be expected since the interior sources are directly coupled to the acoustic medium and hence, the acoustic impedance at the control surface and elsewhere is heavily influenced by the location and distribution on the interior sources.

One now looks at the spatial profile of the specific acoustic impedance in the vicinity of the control elements after control. Please note that since the control elements are rigid rectangular pistons, the velocity over each piston is uniform. Hence the profile of the impedance also reflects the profile of the pressure. Figure 8 shows the specific acoustic

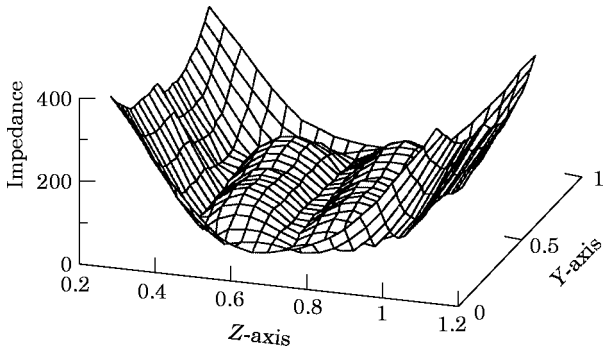


Figure 8. Specific acoustic impedance distribution in the vicinity of the actuators at 180 Hz in the presence of structural disturbances only.

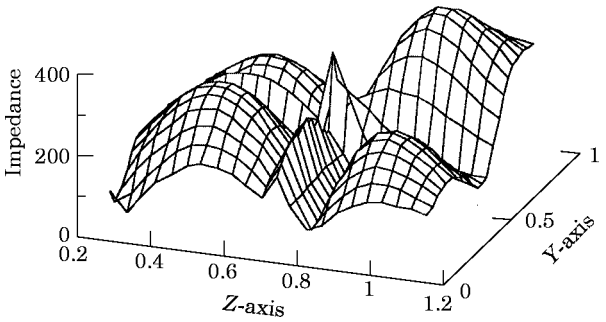


Figure 9. Specific acoustic impedance distribution in the vicinity of the actuators at 180 Hz in the presence of internal point acoustic sources only.

impedance at a sample frequency of 180 Hz when only structural sources cause the primary disturbance (conditions same as in Figure 7). Figure 9 shows the specific acoustic impedance at 180 Hz in the presence of three interior sources. In both cases, we observe a smooth profile over each piston surface within which, the magnitudes of the specific acoustic impedance are close to the value of the acoustic impedance on the control surface at the corresponding frequency. An interesting quantitative observation that can be made regarding the optimal impedance values is that their magnitudes are of the order of the characteristic impedance of air ($Z_{air} = 415\ \mathrm{kg/m^2s}$).

It was also observed that the specific acoustic impedance over the control actuators is purely imaginary. This implies that there is no net power transferred between the control sources and the acoustic medium when the sound field is optimally controlled. This is in agreement with results obtained in reference [4]. This result also suggests that absorption at low frequencies may be accomplished effectively only through active methods.

## 4. CONCLUDING REMARKS

In this paper, extensive simulation results from the impedance modelling of an actively controlled acoustic medium in a three dimensional enclosure have been presented. The acoustic impedance at the control surface, at the interior noise sources, and at the vibrating side wall have been studied. The optimal control has been shown to unload the side wall by reducing the impedance in its vicinity and hence, its acoustic power output. On the other hand, the optimal control may or may not decrease the acoustic power output of interior acoustic sources even though the overall sound pressure level in the enclosure is reduced. If an acoustic source is located near a pressure node before control, the impedance around it may be increased after control resulting in a higher acoustic power output. This suggests that the acoustic source may actually help the controller in reducing the overall sound pressure level.

The acoustic impedance in the vicinity of the control sources is also investigated. It is found that the impedance at the control surface is relatively insensitive to the changes in strength and location of the forces acting on the side wall, whereas it is quite sensitive to the location and distribution of interior acoustic sources. It is also observed that the acoustic impedance on the control surface under optimal control conditions changes significantly with the frequency. This seems to suggest that impedance control in a decentralized or centralized manner may be a viable technique in the case when all the noise in the enclosure is caused by structural vibrations, and that a semi-active approach which

uses a fixed value of impedance over a range of frequencies will be ineffective in suppressing three-dimensional interior noise.

## ACKNOWLEDGMENTS

This work is supported in part by an Individual Investigator Award (IIA) grant (CMS-963467) from the National Science Foundation, and a grant from the State of Delaware Research Partnership program and the Lord Corporation. We would also like to acknowledge the support for Vijay Jayachandran by the University of Delaware Competitive Fellowship.

## REFERENCES

1. K. K. Ahuja and J. C. Stevens 1990 *Proceedings of the* 13*th AIAA*, *Aeroacoustics Conference*, Tallahassee, Fl. Recent advances in active noise control.
2. A. J. Bullmore, P. A. Nelson, A. R. D. Curtis and S. J. Elliott 1987 *Journal of Sound and Vibration* **117**, 15–33. The active minimization of harmonic enclosed sound fields, Part II: a computer simulation.
3. A. J. Bullmore 1987 *Ph.D. Thesis*, *University of Southampton*. The active minimisation of harmonic enclosed sound fields with particular application to propeller induced cabin noise.
4. P. A. Nelson and S. J. Elliott 1992 *Active Control of Sound*. San Diego, CA: Academic Press.
5. J. Tichy 1991 *Journal of Acoustical Society of Japan* (*E*) **12**, 255–262. Current and future issues of active noise control.
6. G. A. Mangiante 1977 *Journal of the Acoustical Society of America* **61**, 1516–1523. Active sound absorption.
7. P. A. Nelson, A. R. D. Curtis and S. J. Elliott 1986 *Proceedings of International Conference on Noise Control Engineering*, *Progress in Noise Control*: *Inter-Noise* 86, Cambridge, MA. 601–606. On the active absorption of sound.
8. Z. Wu, X.-Q. Bao, V. K. Varadan and V. V. Varadan 1993 *Journal of Smart Materials and Structures* **2**, 40–46. Broadband active acoustic absorbing coating with an adaptive digital controller.
9. Z. Wu, V. K. Varadan, V. V. Varadan and K. Y. Lee 1995 *Journal of the Acoustical Society of Amercia* **97**, 1078–1087. Active absorption of acoustic waves using state-space model and optimal control theory.
10. C. J. Radcliffe and S. D. Gogate 1995 *Proceedings of ASME International Mechanical Engineering Congress and Exposition*. An analytical active acoustic sink controller model for wide band noise control applications.
11. P. Darlington and M. R. Avis 1996 *Proceedings of Inter-Noise* 96, Liverpool, England. 1121–1126. Noise control in resonant sound fields using active absorbers.
12. P. Darlington 1996 *Proceedings of Inter-Noise* 96, Liverpool, England. 1127–1131. Active boundary control of enclosed sound fields.
13. X. Meynial 1996 *Proceedings of the third ICIM/ECSSM*'96, Lyon, France. 968–973. Active materials for application in room acoustics.
14. D. Guicking and K. Karcher 1984 *Journal of Vibration*, *Acoustics*, *Stress*, *and Reliability in Design* **106**, 393–396. Active impedance control for one-dimensional sound.
15. F. Marc, T. Denis and G. Marie-Annick 1996 *Proceedings of the Third ICIM/ECSSEM*'96, Lyon, France. 734–739. Actively enhanced porous layers for free field acoustic absorption.
16. O. Lacour, D. Thenail and M. A. Galland 1997 *Proceedings of the Sixteenth Biennial Conference on Mechanical Vibration and Noise*, *ASME Design Engineering Technical Conferences*, Sacramento, California. Actively silencing a cavity by acoustic impedance changes.
17. S. M. Hirsch and J. Q. Sun 1997 *Proceedings of the ASME Sixteenth Biennial Conference on Mechanical Vibration and Noise*, Sacramento, California. Spatial characteristics of acoustic boundary control for interior noise suppression.
18. S. M. Hirsch and J. Q. Sun 1997 *Proceedings of the Eleventh VPI&SU Symposium on Structural Dynamics and Control*, Blacksburg, Virginia. An acoustic boundary control method with actuator grouping for interior noise suppression.
19. J. Q. Sun and S. M. Hirsch 1997 *Proceedings of the SPIE Smart Structures and Materials*'97, San Diego. An acoustic boundary control method for interior noise suppression.

20. V. JAYACHANDRAN, S. M. HIRSCH and J. Q. SUN 1998 *Journal of Sound and Vibration* **210,** 243–254. On the numerical modelling of interior sound fields by the modal function expansion approach.
21. L. L. BERANEK 1993 *Acoustics*. Woodbury, New York: Acoustical Society of America.
22. F. FAHY 1985 *Sound and Structural Vibration*, *Radiation*, *Transmission and Response*. New York: Academic Press.